1	mRNA Degradation Rates Are Coupled to Metabolic Status in <i>Mycobacterium</i>
2	smegmatis
3	
4	Diego A. Vargas-Blanco <sup>a</sup> , Ying Zhou <sup>a</sup> , L. Gregory Zamalloa <sup>a</sup> , Tim Antonelli <sup>b</sup> , Scarlet S.
5	Shell <sup>a,c</sup> #
6	
7	<sup>a</sup> Department of Biology and Biotechnology, Worcester Polytechnic Institute, Worcester,
8	Massachusetts, USA
9	<sup>b</sup> Department of Mathematics, Worcester State University, Worcester, Massachusetts, USA
10	<sup>c</sup> Program in Bioinformatics and Computational Biology, Worcester Polytechnic Institute,
11	Worcester, Massachusetts, USA
12	
13	Running Head: mRNA Stability is Coupled to Metabolic Status
14	
15	#Address correspondence to Scarlet S. Shell, sshell@wpi.edu.
16	
17	Word count: 5,151 words.
18	
19	

#### **ABSTRACT**

20

21

22

23

24

25

26

27

28

29

30

31

32

33

34

35

36

37

38

39

40

The success of *Mycobacterium tuberculosis* (Mtb) as a human pathogen is due in part to its ability to survive stress conditions, such as hypoxia or nutrient deprivation, by entering nongrowing states. In these low-metabolic states, Mtb can tolerate antibiotics and develop genetically encoded antibiotic resistance, making its metabolic adaptation to stress crucial for survival. Numerous bacteria, including Mtb, have been shown to reduce their rates of mRNA degradation under growth limitation and stress. While the existence of this response appears to be conserved across species, the underlying bacterial mRNA stabilization mechanisms remain unknown. To better understand the biology of non-growing mycobacteria, we sought to identify the mechanistic basis of mRNA stabilization in the non-pathogenic model Mycobacterium *smegmatis*. We found that mRNA half-life was responsive to energy stress, with carbon starvation and hypoxia causing global mRNA stabilization. This global stabilization was rapidly reversed when hypoxia-adapted cultures were re-exposed to oxygen, even in the absence of new transcription. The stringent response and RNase levels did not explain mRNA stabilization, nor did transcript abundance. This led us to hypothesize that metabolic changes during growth cessation impact the activity of degradation proteins, increasing mRNA stability. Indeed, bedaquiline and isoniazid, two drugs with opposing effects on cellular energy status, had opposite effects on mRNA half-lives in growth-arrested cells. Taken together, our results indicate that mRNA stability in mycobacteria is not directly regulated by growth status, but rather is dependent on the status of energy metabolism.

#### **IMPORTANCE**

- The logistics of tuberculosis therapy are difficult, requiring multiple drugs for many months. Mtb 41 42
  - survives in part by entering non-growing states in which it is metabolically less active, and thus

less susceptible to antibiotics. Basic knowledge on how Mtb survives during these low-metabolic states is incomplete, and we hypothesize that optimized energy resource management is important. Here we report that slowed mRNA turnover is a common feature of mycobacteria under energy stress, but is not dependent on the mechanisms that have generally been postulated in the literature. Finally, we found that mRNA stability and growth status can be decoupled by a drug that causes growth arrest but increases metabolic activity, indicating that mRNA stability responds to metabolic status rather than to growth rate per se. Our findings suggest a need to reorient studies of global mRNA stabilization to identify novel mechanisms that are presumably responsible.

### **INTRODUCTION**

Most bacteria periodically face environments that are unfavorable for growth. To overcome such challenges, bacteria must tune their gene expression and energy usage. Regulation of mRNA turnover can contribute to both of these. However, the mechanisms by which mRNA turnover is carried out and regulated remain poorly understood, particularly in mycobacteria.

During infection, the human pathogen *Mycobacterium tuberculosis* (Mtb) faces not only the immune response and antibiotics, but also non-optimal microenvironments such as hypoxia and starvation (1, 2). Regulation of mRNA turnover appears to contribute to adaptation to such conditions. A global study of mRNA decay in Mtb showed a dramatic increase in transcriptome stability (increased mRNA half-lives) in response to hypoxia, compared to aerobic growth (3). This suggests that mRNA stabilization contributes to energy conservation in the energy-limited environments that Mtb encounters during infection. Similar responses have been shown for other

bacteria under conditions that slow or halt growth, including carbon deprivation, stationary 65 phase, and temperature shock (4-13). However, the mechanisms responsible for global regulation 66 67 of mRNA stability in prokaryotes remain unknown. A conventional model for RNA decay in E. coli starts with endonucleolytic cleavage by RNase 68 E, particularly in 5' monophosphorylated mRNAs (14-16). The resulting fragments are further 69 70 cleaved by RNase E, producing fragments that are fully degraded by exonucleases such as 71 PNPase, RNase II, and RNase R (17, 18). mRNA degradation is coordinated by formation of a 72 complex known as the degradosome. In E. coli, RNase E serves as the scaffold for degradosomes 73 containing RNA helicases, the glycolytic enzyme enolase, and PNPase (19-23). Other organisms that encode RNase E form similar degradosomes (24, 25). In bacteria lacking RNase E, other 74 endonucleases assume the scaffold function (26-28). Mycobacteria encode RNase E, but efforts 75 76 to define the mycobacterial degradosome have produced inconsistent results (29, 30). It is 77 unclear if degradosome reorganization or dissolution contribute to the global regulation of 78 mRNA degradation in any bacteria. Interestingly, the importance of degradosome formation in E. coli varies depending on the carbon sources provided, suggesting links between RNA 79 degradation and metabolic capabilities (31). Furthermore, the chaperones DnaK and CsdA 80 81 associate with degradosomes in E. coli under certain stresses (20, 32, 33). 82 Global transcript stabilization in stressed bacteria could plausibly result from reduced RNase 83 abundance, reduced RNase activity, and/or reduced accessibility of transcripts to degradation proteins. In E. coli multiple stressors upregulate RNase R, possibly to mitigate ribosome 84 85 misassembly (34, 35), and RNase III levels decrease under cold-shock and stationary phase (36). 86 Surprisingly, protein levels for most putative RNA degradation proteins in Mtb remain unaltered under hypoxic conditions (37), suggesting that mRNA degradation is not necessarily regulated at 87

the level of RNase abundance in mycobacteria. However, there is evidence that RNase activity may be regulated. For example, proteins such as RraA and RraB can alter the function of the RNase E-based degradosome in E. coli (38). Translating ribosomes can mask mRNA cleavage sites and stabilize mRNAs (39). In Caulobacter crescentus, subcellular localization of mRNA degradation proteins may affect global mRNA stability (40, 41). Furthermore, in some actinomycetes, PNPase might be regulated by the stringent response alarmones guanosine-3'diphosphate-5'-triphosphate (pppGpp) and/or guanosine-3',5' -bisphosphate (ppGpp), collectively referred to as (p)ppGpp (42, 43). Many bacteria synthesize (p)ppGpp in response to energy stress (44-47), where it generally facilitates adaptation by upregulating stress-associated genes and downregulating those associated with growth (46, 48-52). (p)ppGpp was reported to inhibit the activity of PNPase in two actinomycetes, Streptomyces coelicolor and Nonomuraea (42, 43), suggesting that the stringent response could directly stabilize mRNA as part of a broader response to energy starvation. Another explanation for stress-induced transcript stabilization could be that reduced transcript abundance directly leads to increased transcript stability. mRNA abundance and half-life were reported to be inversely correlated in multiple bacteria including Mtb (3, 8, 53, 54), and mRNA abundance is lower on a per-cell basis for most transcripts in non-growing bacteria. Nevertheless, the causal relationships between translation, mRNA abundance, RNase expression, and mRNA stability in non-growing bacteria remain largely untested. Given the importance of adaptation to energy starvation for mycobacteria, we sought to investigate the mechanisms by which mRNA stability is globally regulated. Here we show that the global mRNA stabilization response occurs also in *Mycobacterium smegmatis*—a nonpathogenic model commonly used to study the basic biology of mycobacteria —under hypoxia

88

89

90

91

92

93

94

95

96

97

98

99

100

101

102

103

104

105

106

107

108

109

and carbon starvation. Remarkably, we found that hypoxia-induced mRNA stability is rapidly reversible, with re-aeration causing immediate mRNA destabilization even in the absence of protein synthesis. As expected, transcript levels from hypoxic cells were lower on a per-cell basis compared to those from aerated cultures. However, our data are inconsistent with a model in which mRNA abundance dictates degradation rate as has been shown for log-phase *E. coli* (53) and *Lactococcus lactis* (54). Instead, our findings support the idea that mRNA stability is rapidly tuned in response to alterations in energy metabolism. This effect does not require the stringent response or changes in abundance of RNA degradation proteins, and can be decoupled from growth status.

#### RESULTS

mRNA is stabilized as a response to carbon starvation and hypoxic stress in Mycobacterium

# *smegmatis*

The mRNA pools of *E. coli* and other well-studied bacteria were reported to be globally stabilized during conditions of stress, resulting in increased mRNA half-lives (3-13). Rustad *et al.* reported a similar phenomenon in Mtb under hypoxia and cold shock (3). We sought to establish *M. smegmatis* as a model for study of the mechanistic basis of mRNA stabilization in mycobacteria under stress conditions. We therefore subjected *M. smegmatis* to hypoxia and carbon starvation, and measured mRNA half-lives for a subset of genes by blocking transcription with rifampicin (RIF) and measuring mRNA abundance at multiple time-points using quantitative PCR (qPCR). We used a variation of the Wayne model (55) to produce a gradual transition from aerated growth to hypoxia-induced growth arrest by sealing cultures in vials with defined headspace ratios and allowing them to slowly deplete the available oxygen (Fig. 1A-B).

We tested a set of mRNAs that included leadered and leaderless transcripts, monocistronic and polycistronic transcripts, and transcripts with both relatively short and relatively long half-lives in log phase. We observed that all of the analyzed transcripts had increased half-lives under hypoxia when compared to log phase normoxic cultures and, similarly, transcripts were more stable in carbon starvation than in rich media (Fig. 1C-D). Thus, M. smegmatis appears to be a suitable model for investigating the mechanisms of stress-induced mRNA stabilization in mycobacteria. To ensure that the apparent mRNA stabilization was not an artifact of reduced RIF activity in non-growing cells, we confirmed that RIF indeed blocked transcription in hypoxiaarrested M. smegmatis (Fig. 1E). We noted that transcripts became progressively more stable as oxygen levels dropped and growth ceased; 40 hours after sealing the vials, mRNA half-lives were too long to reliably measure by our methodology. We sought to focus our studies on the mechanisms that underlie the initial mRNA stabilization process during the transition into hypoxia-induced growth arrest. We therefore conducted most of our subsequent experiments 18-24 hours after sealing the vials, when growth had nearly ceased and transcripts were 9-fold to 25fold more stable than during log phase. We refer to these conditions as 18 h hypoxia and 24 h hypoxia.

134

135

136

137

138

139

140

141

142

143

144

145

146

147

148

149

150

151

152

153

154

155

156

(p)ppGpp does not contribute to mRNA stabilization in hypoxia or carbon starvation Given recent reports that (p)ppGpp could directly inhibit the enzymatic activity of the exoribonuclease PNPase (42, 43), we wondered whether mRNA stabilization as observed in carbon starvation and hypoxia is regulated by (p)ppGpp in mycobacteria. We obtained a double mutant strain of M. smegmatis (56) that lacks both genes implicated in the production of (p)ppGpp ( $\Delta rel \Delta sas2$ ), and compared the mRNA half-lives of a subset of genes to those of wild type mc<sup>2</sup>155 under hypoxia, log phase normoxia, and carbon starvation. The  $\Delta rel \Delta sas2$  strain

had a growth defect during adaptation to hypoxia and carbon starvation (Fig. 2A and 2C), as predicted (57). However, we found no significant decrease in mRNA stabilization in the mutant strain (Fig. 2B and 2D), indicating that the mRNA stabilization observed under hypoxia and carbon starvation is independent from the stringent response. Interestingly, the mutant strain displayed increased mRNA stabilization for a few transcripts under carbon starvation conditions, which could be an indirect consequence of altered transcription rates (see discussion).

157

158

159

160

161

162

163

164

165

166

167

168

169

170

171

172

173

174

175

176

177

178

179

# Hypoxia-induced mRNA stability is reversible and independent of mRNA abundance

We wondered if the observed stress-induced transcript stabilization could be reversed by restoration of a favorable growth environment. To test this, we prepared 18 h hypoxia cultures, opened the vials and agitated them for 2 min to re-expose the bacteria to oxygen before blocking transcription with RIF and sampling thereafter (Fig. 3A, top). We found that, for all transcripts tested, half-lives were significantly decreased compared to those observed under hypoxia and similar to those observed in log phase (Fig. 3B). While the mechanisms of stress-induced mRNA stabilization are largely unknown, multiple studies have reported inverse correlations between mRNA abundance and half-life in bacteria (3, 8, 53, 54). mRNA abundance was decreased for most transcripts tested in hypoxia-adapted M. smegmatis. We therefore considered the possibility that the dramatic increase in mRNA degradation upon re-exposure to oxygen was triggered by a burst of transcription. Indeed, we found increased expression levels for three of five genes tested after two minutes of re-aeration, showing that transcription is rapidly induced upon return to a favorable environment (Fig. 3C). To test the idea that mRNA is destabilized by re-aeration as a consequence of a transcriptional burst and/or increased mRNA abundance, we modified our reaeration experiment by blocking transcription with RIF one minute prior to re-aeration (Fig. 3A, bottom). Surprisingly, every transcript tested was destabilized by re-aeration despite the absence

of new transcription. For most transcripts, the re-aeration half-lives were indistinguishable regardless of whether RIF was added prior to opening the vials or two minutes after (Fig. 3B). Our results therefore do not support the idea that changes in mRNA abundance alone can explain the mRNA stabilization and destabilization observed in response to changes in energy status. We wanted to further explore if mRNA abundance alone could influence transcript degradation. We obtained a strain encoding *dCas9* and a non-specific sgRNA under control of an ATc-inducible promoter (58) and compared the *dCas9* transcript stability under hypoxia and normoxia after ATc induction or at basal levels. We found that despite a 34-fold transcript upregulation following ATc induction, the half-life of *dCas9* mRNA was not significantly different from the uninduced control in log phase. Under hypoxia, its 28-fold upregulation was associated with an increase in *dCas9* mRNA half-life compared to the no-drug control (Fig. 3D and 3E). Together, our results show that increased mRNA abundance does not necessarily result in a faster decay rate.

# mRNA stability is modulated independently of RNase protein levels

Another potential explanation for increased mRNA degradation after re-aeration is the upregulation of mRNA degradation proteins such as RNase E. To assess the role of a sudden burst in protein levels we used two approaches. First, we constructed strains encoding FLAG-tagged RNase E, cMyc-tagged PNPase, or cMyc-tagged msmeg\_1930 (predicted RNA helicase). We determined protein levels by western blotting in log phase, 18 h hypoxia, and after 18 h hypoxia followed by 2 min re-aeration. Levels of all three of these predicted RNA degradation proteins remained unchanged in the three conditions (Fig. 4A).

Because we do not know all of the proteins that contribute to mRNA degradation in mycobacteria, our second approach was to test the global importance of translation in reaeration-induced mRNA destabilization. We blocked translation with chloramphenicol (CAM) in 18 h hypoxia cultures and then added RIF. Samples were collected for cultures that remained under hypoxia as well as those that were re-aerated for 2 min (Fig. 4B). For three of the five genes tested, we found that CAM caused increased mRNA stability in hypoxia. This is consistent with CAM's mechanism of action and published work (59-61). CAM inhibits elongation by preventing peptidyl transfer (62-64) and causing ribosomal stalling (65). Global stabilization of mRNA pools has been reported when elongation inhibitors, but not initiation inhibitors, are used for example in log phase cultures of E. coli (65) or in yeast (66). We hypothesize that stalled ribosomes may increase mRNA stability by masking RNase cleavage sites. However, despite the stabilization caused by CAM itself, we observed mRNA destabilization in response to reaeration (Fig. 4C). These results suggest that re-aeration-induced destabilization does not require synthesis of new RNA degradation proteins. Taken together, our data suggest that tuning of protein levels is not the primary explanation for mRNA stabilization during early adaptation to hypoxia.

# mRNA stability is modulated in response to changes in metabolic status

201

202

203

204

205

206

207

208

209

210

211

212

213

214

215

216

217

218

219

220

221

222

223

The rapidity of mRNA destabilization following re-aeration suggested that mRNA degradation is tightly regulated in response to changes in energy metabolism. We tested this hypothesis by treating log phase cultures with 5  $\mu$ g·mL<sup>-1</sup> bedaquiline (BDQ), a potent inhibitor of the ATP synthase F<sub>0</sub>F<sub>1</sub> (67). We used minimal media that contained acetate as the only carbon source (MMA) in order to make the respiratory chain the sole source of ATP synthesis. After 30 min exposure, intracellular ATP levels were reduced by more than 90% compared to cells treated

with vehicle (DMSO), without affecting viability (Fig. 5A and 5B). We then measured half-lives for a set of transcripts under these conditions. mRNA half-lives were dramatically increased in BDQ-treated cells for most of the genes we tested (Fig. 5C), indicating that mRNA degradation rates are rapidly altered in response to changes in energy metabolism status. We then wondered if we could increase mRNA degradation rates by increasing intracellular ATP levels. To test this, we treated *M. smegmatis* cultures with isoniazid (INH) a pro-drug that interferes with the synthesis of mycolic acids, and also leads to an accumulation of intracellular ATP due to increased oxidative phosphorylation (68). We exposed M. smegmatis to 500 µg·mL<sup>-1</sup> INH for 6.5 hours to confirm that we had achieved bacteriostasis (M. smegmatis doubling time in MMA media is ~six hours). As shown in Fig. 5D, INH caused a dramatic increase in intracellular ATP after 6.5 h without affecting cell viability (Fig. 5E). Remarkably, mRNA halflives were significantly decreased in response to INH (Fig. 5F). To our knowledge, this is the first report of bacterial mRNA being destabilized rather than stabilized in response to a growthimpairing stressor. Our results indicate that mRNA stability is regulated not in response to growth status per se, but rather to energy metabolism. Although we interpreted ATP levels as a reflection of metabolic status in our INH and BDQ assays, the coupling between mRNA degradation and metabolic status does not appear to be mediated by ATP directly. We measured ATP levels in cultures during the transition to hypoxia-induced growth arrest, and found that although ATP levels ultimately decrease in hypoxia as has been reported elsewhere (69, 70), mRNA stabilization precedes the drop in ATP levels (Fig. 5G).

244

245

224

225

226

227

228

229

230

231

232

233

234

235

236

237

238

239

240

241

242

243

# **DISCUSSION**

Stressors that cause bacteria to slow or stop growth are typically associated with increased mRNA stability (3-9, 11-13). Many of these same stressors reduce energy availability (69, 70), requiring reductions in energy consumption and optimization of resource allocation. We speculate that the decreased mRNA turnover that accompanies such conditions may be an energy conservation mechanism. For Mtb, hypoxia can lead to generation of bacterial subpopulations with varying degrees of antibiotic tolerance (71-73), facilitating bacterial survival and the acquisition of drug resistance-conferring mutations. Understanding the mechanisms that support the transitions into non-growing states, and subsequent survival in these states, is therefore a priority. The transcriptome of Mtb has been shown to be stabilized under cold shock and hypoxia (3). Here, we found that *M. smegmatis* also dramatically stabilized its mRNA in response to carbon starvation and hypoxia. For the first time, to our knowledge, we tested the speed at which this stabilization is reversed in mycobacteria upon restoration of energy availability. Remarkably, mRNAs are rapidly destabilized within minutes of re-aeration of hypoxic cultures, suggesting that tuning of mRNA degradation rates is an early step in the response to changing energy availability. The most straightforward explanation for stress-induced mRNA stabilization would seem to be downregulation of the mRNA degradation machinery. Indeed, RNase E is downregulated at the transcript level under hypoxia, and abundance of cleaved RNAs is reduced (74). However, we found that protein levels were unchanged for RNase E and two other proteins predicted to be core components of the mRNA degradation machinery. This is largely consistent with what was reported for Mtb in a quantitative proteomics study (37), although in that case there was an apparent reduction in levels of an RNA helicase. To address this question in a more agnostic

246

247

248

249

250

251

252

253

254

255

256

257

258

259

260

261

262

263

264

265

266

267

fashion, we tested the importance of translation for transcript destabilization upon re-exposure of hypoxic cultures to oxygen. However, re-aeration triggered increased transcript degradation even in the absence of new protein synthesis. Regulation of degradation protein levels therefore does not appear to contribute to mRNA stabilization during the initial response to energy stress. However, we found that upon longer periods of hypoxia, transcripts were stabilized to a greater extent than what we observed 18 hours after sealing the vials. This suggests that mRNA stabilization progressively increases, and may involve multiple mechanisms. As this work focused on the initial transition into hypoxia-induced growth arrest, we cannot discount the possibility that downregulation of the RNA degradation machinery is important for further mRNA stabilization in later hypoxia stages. Interestingly, we found greater mRNA stabilization in hypoxic cultures treated with CAM. This may result from stalled ribosomes (62, 64) masking RNase cleavage sites. Furthermore, the burst of transcription upon re-aeration is blocked by the presence of CAM, causing up to a four-fold decrease in transcript abundance in the CAM treated cultures when compared to the vehicle treated cultures. This is consistent with the idea that transcription and translation are physically coupled, and blocking translation therefore prevents RNA polymerase from efficiently carrying out transcript elongation, as was reported for E. coli (75-79). The results obtained from the  $\Delta rel$  $\Delta sas2$  strain are also consistent with the idea that the presence of ribosomes affects mRNA stability. Under carbon starvation this strain had rRNA levels three-fold higher than the WT strain, consistent with the known role of (p)ppGpp in downregulating ribosome biogenesis (80-82). Interestingly, some transcripts were hyperstabilized in the  $\Delta rel \Delta sas2$  strain under carbon starvation, showing virtually no degradation (Fig. 2D). We speculate that the observed mRNA hyperstabilization could be the caused by increased ribosome abundance, resulting in augmented

269

270

271

272

273

274

275

276

277

278

279

280

281

282

283

284

285

286

287

288

289

290

mRNA-ribosome associations that ultimately protect transcripts from RNases. Alternatively, the increased abundance of rRNA could protect mRNA indirectly by providing alternative targets that compete for interaction with RNases (65).

Transcript abundance has been found to be inversely correlated with mRNA stability in exponentially growing bacteria (3, 8, 53, 54, 83), and experimental manipulation of transcription rates of subsets of genes affected their degradation rates (3, 54). Together, these studies suggest that high rates of transcription inherently increase degradation rates. We report here that during oxygen depletion transcript levels are reduced in *M. smegmatis*, which led us to ask if increased transcript half-lives under stress are a direct result of reduced mRNA levels. However, our data are inconsistent with this idea; mRNA is rapidly destabilized upon re-aeration even in the absence of new transcription. We note that one study reported a weak positive correlation between mRNA abundance and stability in log phase *E. coli* (12), while another reported mRNA abundance to be positively correlated with stability in carbon-starved *Lactococcus lactis* (8). Together, these observations and our own suggest that the relationship between mRNA stability and abundance is not yet fully understood and may be fundamentally different in growth-arrested bacteria.

The rapid reversibility of hypoxia-induced mRNA stabilization suggests that mRNA decay and energy metabolic status are closely linked. Consistent with this, we have shown that drug-induced energy stress causes mRNA stabilization, while mRNA decay is increased by a drug that induces a hyperactive metabolic state. To our knowledge this is the first demonstration that the rate of bacterial mRNA degradation can be decoupled from growth rate, and suggests that mRNA decay is controlled by energy status rather than growth rate per se. The mechanism by which energy status and mRNA decay are coupled remains elusive; the stringent response is not

required, and the stabilization of mRNA during adaptation to hypoxia precedes a decrease in ATP levels. Our data are consistent with two general (non-exclusive) models: mRNA decay could be regulated by protection of transcripts from RNase attack, and/or by direct regulation of the activity of the RNases. Possible explanations that fall within one or both of these frameworks include changes in ribosome occupancy, the presence of other RNA-binding proteins, regulation of the subcellular localization of mRNAs and/or the RNA degradation machinery, and altered degradosome composition. These possibilities should be investigated in future work.

#### **METHODS**

# Strains and culture conditions

*Mycobacterium smegmatis* strain mc<sup>2</sup>155 or derivatives (Table 1) were grown in *rich medium*, Middlebrook 7H9 with ADC (Albumin Dextrose Catalase, final concentrations 5 g·L<sup>-1</sup> BSA fraction V [BSA], 2 g·L<sup>-1</sup> dextrose, 0.85 g·L<sup>-1</sup> NaCl, and 3 mg·L<sup>-1</sup> catalase), 0.2% glycerol and 0.05% Tween 80 at 200 rpm and 37°C to an OD<sub>600</sub> of ~0.8, unless specified otherwise. For hypoxic cultures, we modified the Wayne model (55). Bacteria were cultured in 30.5 x 58 mm serum bottles (Wheaton, 223687, 20 mL) using *rich medium* and an initial OD<sub>600</sub>=0.01. Bottles were sealed with a vial crimper (Wheaton, W225303) using rubber stoppers (Wheaton, W224100-181) and aluminum seals (Wheaton, 224193-01). Oxygen levels were qualitatively monitored using methylene blue.

BSA, 0.85 g·L<sup>-1</sup> NaCl, 3 mg·L<sup>-1</sup> catalase, and 0.05 % Tyloxapol) at 4°C, then resuspended in *carbon starvation medium* to OD<sub>600</sub>= 0.8 and incubated at 200 rpm, 37°C.

The RNase E-tagged strain (SS-M\_0296) was built using a two-step process. Plasmid pSS250 was derived from pJM1 (84) and contained 1 kb of the sequence upstream and downstream of the *rne* (msmeg\_4626) start codon, with the sequence encoding 6xHis-3xFLAG-TEV-4xGly inserted after the start codon. Constructs were built using NEBuilder HiFi (E2621). Integrants were selected with 200 μg·mL<sup>-1</sup> hygromycin and confirmed by sequencing. Counter-selection with 15% sucrose was followed by PCR screening to identify isolates that underwent second

The PNPase-tagged strain (SS-M\_0412) was built by inserting a second copy of *pnp* (msmeg\_2656) with an N-terminal c-Myc-4xGly and its predicted native promoter and 5' UTR at the Giles phage integration site (plasmid pSS282) into strain SS-M\_0296. The RNA helicase-tagged strain (SS-M\_0416) was constructed in a similar way but using a C-terminal 4xGly-c-Myc tag on msmeg\_1930 (plasmid pSS285).

# RNA extraction and determination of mRNA stability

crossovers resulting in loss of the plasmid and retention of tagged *rne*.

Biological triplicate cultures were treated with rifampicin (RIF) to a final concentration of 150 μg·mL<sup>-1</sup> to halt transcription and RNA was extracted at various time-points thereafter. For exponential and carbon starvation cultures, 7 mL were collected per replicate and time-point and snap-frozen in liquid nitrogen (LN2). For hypoxic samples, degassed RIF was injected using a 30G needle, and all samples were sacrificially collected per time-point and replicate (7 mL) and snap-frozen in LN2 within 6 seconds of unsealing.

Samples were stored at -80°C and thawed on ice immediately before RNA extraction. Cells were pelleted at 4°C, resuspended in 1 mL TRIzol (Invitrogen), transferred to 2 mL disruption tubes (OPS Diagnostics 100 µm zirconium lysing matrix, molecular grade), and lysed using a FastPrep-24 5G (MP) (3 cycles of 7 m·s<sup>-1</sup> for 30 s, 2 min on ice between cycles). 300 μL chloroform was added, samples centrifuged 15 min at 21,130 x g and 4°C, and RNA recovered from the aqueous layer and purified with a Direct-zol RNA MiniPrep kit according to the manufacturer's instructions with in-column DNase treatment. Agarose gels were used to verify RNA integrity. For cDNA synthesis, 600 ng of total RNA were mixed with 0.83 µL 100 mM tris pH 7.5 and 0.17 μL 3 mg·mL<sup>-1</sup> Random Primers (NEB) in 5.25 μL, denatured at 70°C for 10 min and snapcooled. Reverse transcription was performed for 5 hours at 42°C using 100 U ProtoScript® II Reverse Transcriptase (NEB), 10 U RNase Inhibitor (Murine, NEB), 0.5 mM each dNTP mix and 5 mM DTT in a final volume of 10 µL. RNA was degraded with 5 µL each 0.5 mM EDTA and 1 N NaOH at 65°C for 15 min, followed by 12.5 uL of 1 M Tris-HCl pH 7.5. cDNA was purified using the MinElute PCR Purification Kit (Qiagen) according to the manufacturer instructions. mRNA abundance (A) over time (t) was determined for different genes (primers in Table 2) by quantitative PCR (qPCR) using iTaq SYBR Green (Bio-Rad) with 400 pg of cDNA and 0.25 µM each primer in 10 µL reactions, with 40 cycles of 15 s at 95°C and 1 min at 61°C (Applied Biosystems 7500). Abundance was expressed as the - $C_T$  (reflecting the  $log_2A(t)$ ). Linear regression was performed on -C<sub>T</sub> values versus time where the negative reciprocal of the best-fit slope estimates mRNA half-life (see supplemental materials, Text S1 and Fig. S1). In many cases the decay curves were biphasic, with a rapid period of decay followed by a period of

357

358

359

360

361

362

363

364

365

366

367

368

369

370

371

372

373

374

375

376

377

slow or undetectable decay. In these cases, only the initial, steeper slope was used for calculation of half-lives.

# mRNA stability during re-aeration and translational inhibition

Translation was halted by 150 μg·mL<sup>-1</sup> chloramphenicol, rifampicin was added 1 min later, and samples collected starting 1 min after that. For re-aeration experiments, 18 h hypoxia cultures were opened, the contents transferred to 50 mL conical tubes, and triplicate samples taken 2, 7, 12, 17, and 32 min after opening the bottles and snap-frozen in LN2. Rifampicin was added either 1 min before (transcription inhibition during hypoxia) or 2 min after opening the bottles (transcription inhibition after re-aeration).

# Bedaquiline and isoniazid treatments

Cultures were grown to OD<sub>600</sub> ~1.0 in *rich medium*, rinsed twice in *Minimal Media Acetate wash* (final concentrations: 0.5 g·L<sup>-1</sup> L-asparagine, 1 g·L<sup>-1</sup> KH<sub>2</sub>PO<sub>4</sub>, 2.5 g·L<sup>-1</sup> Na<sub>2</sub>HPO<sub>4</sub>, 0.5 g·L<sup>-1</sup> MgSO<sub>4</sub>•7H<sub>2</sub>O, 0.5 mg·L<sup>-1</sup> CaCl<sub>2</sub>, 0.1 mg·L<sup>-1</sup> ZnSO<sub>4</sub>, 0.1% CH<sub>3</sub>COONa, 0.05% tyloxapol, pH 7.5) at 4°C, resuspended in Minimal Media Acetate with ferric ammonium citrate (MMA, *Minimal Media Acetate wash* + 50 mg·L<sup>-1</sup> ferric ammonium citrate) to OD<sub>600</sub>=0.07, and grown for 24 hours to OD<sub>600</sub> ~0.8. To remove the extracellular ATP, 30 minutes before drug treatment cells were pelleted and rinsed in pre-warmed *Minimal Media Acetate wash*, resuspended in pre-warmed MMA, and returned to the incubator. Bedaquiline (BDQ), isoniazid (INH), or their vehicles were added to final concentrations of 5 μg·mL<sup>-1</sup> or 500 μg·mL<sup>-1</sup>, respectively. Samples were taken 30 min after adding BDQ, or 6.5 h after adding INH for half-life and ATP determination.

For half-life measurements, BDQ cultures were sampled 0, 3, 6, 9, 12, 15 and 21 min after adding RIF and INH cultures were sampled 0, 4, 8 and 12 min after adding RIF. RNA extractions were performed as above with the following modifications: cell disruption was performed using 2 mL tubes prefilled with Lysing Matrix B (MP) and 3 cycles of 10 m·s<sup>-1</sup> for 40 s; RNA was recovered from the aqueous layer by isopropanol precipitation and resuspension in H<sub>2</sub>O; samples were treated with 5 U of TURBO<sup>TM</sup> DNase (Ambion) in presence of 80 U of RNase Inhibitor, Murine (NEB) for 1 hour at 37°C with agitation. RNA was purified with an RNeasy Mini Kit (Qiagen) according to the manufacturer's specifications.

# **Intracellular ATP estimation**

ATP was estimated by BacTiter-Glo (Promega). For BDQ or INH treatments, 1 mL of culture was pelleted at ~21°C for 1 min at 21,130 x g, the supernatant removed and cells resuspended in 1 mL of pre-warmed MMA containing BDQ, INH, or vehicle to match the prior treatment condition. Immediately after, 20  $\mu$ L samples were transferred to a white 384-well plate (Greiner bio-one) containing 80  $\mu$ L of BacTiter-Glo reagent and mixed for 5 minutes at room temperature. Luminescence was measured in a VICTOR³ plate reader (PerkinElmer) (intracellular ATP). We included controls for the supernatant collected (extracellular ATP), media + drug/vehicle (background), and ATP standards for constructing standard curves.

To estimate intracellular ATP in normoxia and hypoxia cultures, 20  $\mu$ L samples were collected at 37°C and immediately combined with the reagent to measure total ATP (intracellular + extracellular). From the same cultures, 1 mL samples were syringe-filtered (PES 0.2  $\mu$ m) and the filtrate combined with the reagent to measure extracellular ATP. Luminescence was measured as above. Intracellular ATP was calculated by subtracting the extracellular ATP values from the

total ATP values. Hypoxia samples were sacrificially harvested per time-point/replicate and 422 combined with the reagent in <6 seconds. 423 424 **AUTHOR CONTRIBUTIONS** 425 426 DVB and SSS conceived and designed the experiments. DVB and YZ performed the experiments. LGZ performed part of the experiments in Fig. 3. DVB, TA and SSS analyzed the 427 data. DVB and SSS wrote the manuscript. 428 429 **ACKNOWLEDGEMENTS** 430 431 This work was supported by NSF CAREER award 1652756 to SSS. DVB was partially supported by the LASPAU Fulbright Foreign Student Program. We thank all members of the Shell lab for 432 technical assistance and helpful discussions. We thank Dr. Christina Stallings, Dr. Jeremy Rock, 433 and Dr. Sarah Fortune for generously providing strains. 434 435 References 436 Via LE, Lin PL, Ray SM, Carrillo J, Allen SS, Eum SY, Taylor K, Klein E, Manjunatha U, Gonzales J, 437 1. Lee EG, Park SK, Raleigh JA, Cho SN, McMurray DN, Flynn JL, Barry CE, 3rd. 2008. Tuberculous 438 439 granulomas are hypoxic in guinea pigs, rabbits, and nonhuman primates. Infect Immun 76:2333-40. 440 Belton M, Brilha S, Manavaki R, Mauri F, Nijran K, Hong YT, Patel NH, Dembek M, Tezera L, 441 2. Green J, Moores R, Aigbirhio F, Al-Nahhas A, Fryer TD, Elkington PT, Friedland JS. 2016. Hypoxia 442 443 and tissue destruction in pulmonary TB. Thorax 71:1145-1153. Rustad TR, Minch KJ, Brabant W, Winkler JK, Reiss DJ, Baliga NS, Sherman DR. 2013. Global 444 3. 445 analysis of mRNA stability in Mycobacterium tuberculosis. Nucleic Acids Res 41:509-17.

Albertson MH, Nyström T, Kjelleberg S. 1990. Functional mRNA half-lives in the marine Vibrio sp.

S14 during starvation and recovery. Microbiology 136:2195-2199.

446

447

4.

- Georgellis D, Barlow T, Arvidson S, von Gabain A. 1993. Retarded RNA turnover in *Escherichia coli*: a means of maintaining gene expression during anaerobiosis. Mol Microbiol 9:375-81.
- 450 6. Sakamoto T, Bryant DA. 1997. Temperature-regulated mRNA accumulation and stabilization for
   451 fatty acid desaturase genes in the cyanobacterium *Synechococcus* sp. strain PCC 7002. Mol
   452 Microbiol 23:1281-92.
- Thorne SH, Williams HD. 1997. Adaptation to nutrient starvation in *Rhizobium leguminosarum* bv. phaseoli: analysis of survival, stress resistance, and changes in macromolecular synthesis during entry to and exit from stationary phase. J Bacteriol 179:6894-901.
- 456 8. Redon E, Loubiere P, Cocaign-Bousquet M. 2005. Role of mRNA stability during genome-wide adaptation of *Lactococcus lactis* to carbon starvation. J Biol Chem 280:36380-5.
- 458 9. Anderson KL, Roberts C, Disz T, Vonstein V, Hwang K, Overbeek R, Olson PD, Projan SJ, Dunman 459 PM. 2006. Characterization of the *Staphylococcus aureus* heat shock, cold shock, stringent, and 460 SOS responses and their effects on log-phase mRNA turnover. J Bacteriol 188:6739-56.
- Dressaire C, Picard F, Redon E, Loubiere P, Queinnec I, Girbal L, Cocaign-Bousquet M. 2013. Role
   of mRNA stability during bacterial adaptation. PLoS One 8:e59059.
- 463 11. Esquerre T, Laguerre S, Turlan C, Carpousis AJ, Girbal L, Cocaign-Bousquet M. 2014. Dual role of 464 transcription and transcript stability in the regulation of gene expression in *Escherichia coli* cells 465 cultured on glucose at different growth rates. Nucleic Acids Res 42:2460-72.
- 466 12. Chen H, Shiroguchi K, Ge H, Xie XS. 2015. Genome-wide study of mRNA degradation and transcript elongation in *Escherichia coli*. Mol Syst Biol 11:781.
- Ignatov DV, Salina EG, Fursov MV, Skvortsov TA, Azhikina TL, Kaprelyants AS. 2015. Dormant
   non-culturable *Mycobacterium tuberculosis* retains stable low-abundant mRNA. BMC Genomics
   16:954.
- Tomcsanyi T, Apirion D. 1985. Processing enzyme ribonuclease E specifically cleaves RNA I. An inhibitor of primer formation in plasmid DNA synthesis. J Mol Biol 185:713-20.
- 473 15. Bouvet P, Belasco JG. 1992. Control of RNase E-mediated RNA degradation by 5'-terminal base pairing in *E. coli*. Nature 360:488-91.
- 475 16. McDowall KJ, Lin-Chao S, Cohen SN. 1994. A+U content rather than a particular nucleotide order determines the specificity of RNase E cleavage. J Biol Chem 269:10790-6.
- 477 17. Apirion D, Gitelman DR. 1980. Decay of RNA in RNA processing mutants of *Escherichia coli*. Mol 478 Gen Genet 177:339-43.
- Donovan WP, Kushner SR. 1986. Polynucleotide phosphorylase and ribonuclease II are required for cell viability and mRNA turnover in *Escherichia coli* K-12. Proc Natl Acad Sci U S A 83:120-4.
- 481 19. Py B, Causton H, Mudd EA, Higgins CF. 1994. A protein complex mediating mRNA degradation in *Escherichia coli*. Mol Microbiol 14:717-29.
- 483 20. Miczak A, Kaberdin VR, Wei CL, Lin-Chao S. 1996. Proteins associated with RNase E in a multicomponent ribonucleolytic complex. Proc Natl Acad Sci U S A 93:3865-9.
- 485 21. Py B, Higgins CF, Krisch HM, Carpousis AJ. 1996. A DEAD-box RNA helicase in the *Escherichia coli* 486 RNA degradosome. Nature 381:169-72.
- 487 22. Grunberg-Manago M. 1999. Messenger RNA stability and its role in control of gene expression in bacteria and phages. Annu Rev Genet 33:193-227.
- 489 23. Carpousis AJ, Van Houwe G, Ehretsmann C, Krisch HM. 1994. Copurification of *E. coli* RNAase E
   490 and PNPase: evidence for a specific association between two enzymes important in RNA
   491 processing and degradation. Cell 76:889-900.
- 492 24. Vanzo NF, Li YS, Py B, Blum E, Higgins CF, Raynal LC, Krisch HM, Carpousis AJ. 1998. Ribonuclease
   493 E organizes the protein interactions in the *Escherichia coli* RNA degradosome. Genes Dev
   494 12:2770-81.

- 495 25. Ait-Bara S, Carpousis AJ. 2010. Characterization of the RNA degradosome of *Pseudoalteromonas* 496 *haloplanktis*: conservation of the RNase E-RhlB interaction in the gammaproteobacteria. J
   497 Bacteriol 192:5413-23.
- Commichau FM, Rothe FM, Herzberg C, Wagner E, Hellwig D, Lehnik-Habrink M, Hammer E,
   Volker U, Stulke J. 2009. Novel activities of glycolytic enzymes in *Bacillus subtilis*: interactions with essential proteins involved in mRNA processing. Mol Cell Proteomics 8:1350-60.
- 501 27. Roux CM, DeMuth JP, Dunman PM. 2011. Characterization of components of the *Staphylococcus* aureus mRNA degradosome holoenzyme-like complex. J Bacteriol 193:5520-6.
- Redko Y, Aubert S, Stachowicz A, Lenormand P, Namane A, Darfeuille F, Thibonnier M, De Reuse
   H. 2013. A minimal bacterial RNase J-based degradosome is associated with translating
   ribosomes. Nucleic Acids Res 41:288-301.
- 506 29. Kovacs L, Csanadi A, Megyeri K, Kaberdin VR, Miczak A. 2005. Mycobacterial RNase E-associated proteins. Microbiol Immunol 49:1003-7.
- 508 30. Csanadi A, Faludi I, Miczak A. 2009. MSMEG\_4626 ribonuclease from *Mycobacterium* 509 smegmatis. Mol Biol Rep 36:2341-4.
- 510 31. Tamura M, Moore CJ, Cohen SN. 2013. Nutrient dependence of RNase E essentiality in Escherichia coli. J Bacteriol 195:1133-41.
- 512 32. Prud'homme-Genereux A, Beran RK, Iost I, Ramey CS, Mackie GA, Simons RW. 2004. Physical and functional interactions among RNase E, polynucleotide phosphorylase and the cold-shock protein, CsdA: evidence for a 'cold shock degradosome'. Mol Microbiol 54:1409-21.
- Regonesi ME, Del Favero M, Basilico F, Briani F, Benazzi L, Tortora P, Mauri P, Deho G. 2006.
   Analysis of the *Escherichia coli* RNA degradosome composition by a proteomic approach.
   Biochimie 88:151-61.
- 518 34. Chen C, Deutscher MP. 2005. Elevation of RNase R in response to multiple stress conditions. J 519 Biol Chem 280:34393-6.
- 520 35. Chen C, Deutscher MP. 2010. RNase R is a highly unstable protein regulated by growth phase and stress. RNA 16:667-72.
- 522 36. Kim KS, Manasherob R, Cohen SN. 2008. YmdB: a stress-responsive ribonuclease-binding regulator of *E. coli* RNase III activity. Genes Dev 22:3497-508.
- Schubert OT, Ludwig C, Kogadeeva M, Zimmermann M, Rosenberger G, Gengenbacher M, Gillet
   LC, Collins BC, Rost HL, Kaufmann SH, Sauer U, Aebersold R. 2015. Absolute Proteome
   Composition and Dynamics during Dormancy and Resuscitation of *Mycobacterium tuberculosis*.
   Cell Host Microbe 18:96-108.
- 38. Gao J, Lee K, Zhao M, Qiu J, Zhan X, Saxena A, Moore CJ, Cohen SN, Georgiou G. 2006.
   Differential modulation of *E. coli* mRNA abundance by inhibitory proteins that alter the
- composition of the degradosome. Mol Microbiol 61:394-406.
- 531 39. lost I, Guillerez J, Dreyfus M. 1992. Bacteriophage T7 RNA polymerase travels far ahead of ribosomes *in vivo*. J Bacteriol 174:619-22.
- 533 40. Russell JH, Keiler KC. 2009. Subcellular localization of a bacterial regulatory RNA. Proc Natl Acad Sci U S A 106:16405-9.
- 535 41. Bayas CA, Wang J, Lee MK, Schrader JM, Shapiro L, Moerner WE. 2018. Spatial organization and dynamics of RNase E and ribosomes in *Caulobacter crescentus*. Proc Natl Acad Sci U S A 115:E3712-E3721.
- 538 42. Gatewood ML, Jones GH. 2010. (p)ppGpp inhibits polynucleotide phosphorylase from 539 streptomyces but not from *Escherichia coli* and increases the stability of bulk mRNA in 540 *Streptomyces coelicolor*. J Bacteriol 192:4275-80.

- Siculella L, Damiano F, di Summa R, Tredici SM, Alduina R, Gnoni GV, Alifano P. 2010. Guanosine
   5'-diphosphate 3'-diphosphate (ppGpp) as a negative modulator of polynucleotide
   phosphorylase activity in a 'rare' actinomycete. Mol Microbiol 77:716-29.
- 544 44. Frederix M, Downie AJ. 2011. Quorum sensing: regulating the regulators. Adv Microb Physiol 58:23-80.
- 546 45. Atkinson GC, Tenson T, Hauryliuk V. 2011. The RelA/SpoT homolog (RSH) superfamily: 547 distribution and functional evolution of ppGpp synthetases and hydrolases across the tree of 548 life. PLoS One 6:e23479.
- Corrigan RM, Bellows LE, Wood A, Grundling A. 2016. ppGpp negatively impacts ribosome
   assembly affecting growth and antimicrobial tolerance in Gram-positive bacteria. Proc Natl Acad
   Sci U S A 113:E1710-9.
- 552 47. Battesti A, Bouveret E. 2006. Acyl carrier protein/SpoT interaction, the switch linking SpoT-553 dependent stress response to fatty acid metabolism. Mol Microbiol 62:1048-63.
- Gentry DR, Hernandez VJ, Nguyen LH, Jensen DB, Cashel M. 1993. Synthesis of the stationaryphase sigma factor sigma s is positively regulated by ppGpp. J Bacteriol 175:7982-9.
- Chakraburtty R, Bibb M. 1997. The ppGpp synthetase gene (relA) of *Streptomyces coelicolor* A3(2) plays a conditional role in antibiotic production and morphological differentiation. J
   Bacteriol 179:5854-61.
- 559 50. Martinez-Costa OH, Fernandez-Moreno MA, Malpartida F. 1998. The relA/spoT-homologous 560 gene in *Streptomyces coelicolor* encodes both ribosome-dependent (p)ppGpp-synthesizing and -561 degrading activities. J Bacteriol 180:4123-32.
- 562 51. Artsimovitch I, Patlan V, Sekine S, Vassylyeva MN, Hosaka T, Ochi K, Yokoyama S, Vassylyev DG. 2004. Structural basis for transcription regulation by alarmone ppGpp. Cell 117:299-310.
- 564 52. Avarbock D, Avarbock A, Rubin H. 2000. Differential regulation of opposing Rel<sub>Mtb</sub> activities by the aminoacylation state of a tRNA.ribosome.mRNA.Rel<sub>Mtb</sub> complex. Biochemistry 39:11640-8.
- 566 53. Bernstein JA, Khodursky AB, Lin PH, Lin-Chao S, Cohen SN. 2002. Global analysis of mRNA decay
   567 and abundance in *Escherichia coli* at single-gene resolution using two-color fluorescent DNA
   568 microarrays. Proc Natl Acad Sci U S A 99:9697-702.
- 569 54. Nouaille S, Mondeil S, Finoux AL, Moulis C, Girbal L, Cocaign-Bousquet M. 2017. The stability of
   570 an mRNA is influenced by its concentration: a potential physical mechanism to regulate gene
   571 expression. Nucleic Acids Res 45:11711-11724.
- 572 55. Wayne LG, Hayes LG. 1996. An *in vitro* model for sequential study of shiftdown of
   573 *Mycobacterium tuberculosis* through two stages of nonreplicating persistence. Infect Immun
   574 64:2062-9.
- 575 56. Weiss LA, Stallings CL. 2013. Essential roles for *Mycobacterium tuberculosis* Rel beyond the production of (p)ppGpp. J Bacteriol 195:5629-38.
- 57. Dahl JL, Arora K, Boshoff HI, Whiteford DC, Pacheco SA, Walsh OJ, Lau-Bonilla D, Davis WB, Garza AG. 2005. The relA homolog of *Mycobacterium smegmatis* affects cell appearance, viability, and gene expression. J Bacteriol 187:2439-47.
- 58. Rock JM, Hopkins FF, Chavez A, Diallo M, Chase MR, Gerrick ER, Pritchard JR, Church GM, Rubin 581 EJ, Sassetti CM, Schnappinger D, Fortune SM. 2017. Programmable transcriptional repression in 582 mycobacteria using an orthogonal CRISPR interference platform. Nat Microbiol 2:16274.
- 583 59. Shaila MS, Gopinathan KP, Ramakrishnan T. 1973. Protein synthesis in *Mycobacterium*584 *tuberculosis* H37Rv and the effect of streptomycin in streptomycin-susceptible and -resistant
  585 strains. Antimicrob Agents Chemother 4:205-13.
- 586 60. Wu ML, Tan J, Dick T. 2015. Eagle Effect in Nonreplicating Persister Mycobacteria. Antimicrob 587 Agents Chemother 59:7786-9.

- 588 61. Srivastava A, Asahara H, Zhang M, Zhang W, Liu H, Cui S, Jin Q, Chong S. 2016. Reconstitution of Protein Translation of Mycobacterium Reveals Functional Conservation and Divergence with the Gram-Negative Bacterium *Escherichia coli*. PLoS One 11:e0162020.
- Wolfe AD, Hahn FE. 1965. Mode of Action of Chloramphenicol. IX. Effects of Chloramphenicol
   Upon a Ribosomal Amino Acid Polymerization System and Its Binding to Bacterial Ribosome.
   Biochim Biophys Acta 95:146-55.
- 594 63. Yukioka M, Morisawa S. 1971. Enhancement of the phenylalanyl-oligonucleotide binding to the 595 peptidyl recognition center of ribosomal peptidyltransferase and inhibition of the 596 chloramphenicol binding to ribosomes. Biochim Biophys Acta 254:304-15.
- 597 64. Drainas D, Kalpaxis DL, Coutsogeorgopoulos C. 1987. Inhibition of ribosomal peptidyltransferase 598 by chloramphenicol. Kinetic studies. Eur J Biochem 164:53-8.
- Lopez PJ, Marchand I, Yarchuk O, Dreyfus M. 1998. Translation inhibitors stabilize *Escherichia coli* mRNAs independently of ribosome protection. Proc Natl Acad Sci U S A 95:6067-72.
- 601 66. Chan LY, Mugler CF, Heinrich S, Vallotton P, Weis K. 2018. Non-invasive measurement of mRNA decay reveals translation initiation as the major determinant of mRNA stability. eLife 7.
- 603 67. Lakshmanan M, Xavier AS. 2013. Bedaquiline The first ATP synthase inhibitor against multi drug resistant tuberculosis. J Young Pharm 5:112-5.
- 605 68. Shetty A, Dick T. 2018. Mycobacterial Cell Wall Synthesis Inhibitors Cause Lethal ATP Burst. Front Microbiol 9:1898.
- 607 69. Rao SP, Alonso S, Rand L, Dick T, Pethe K. 2008. The protonmotive force is required for maintaining ATP homeostasis and viability of hypoxic, nonreplicating *Mycobacterium tuberculosis*. Proc Natl Acad Sci U S A 105:11945-50.
- 610 70. Eoh H, Rhee KY. 2013. Multifunctional essentiality of succinate metabolism in adaptation to hypoxia in *Mycobacterium tuberculosis*. Proc Natl Acad Sci U S A 110:6554-9.
- 512 571. Smith T, Wolff KA, Nguyen L. 2013. Molecular biology of drug resistance in *Mycobacterium tuberculosis*. Curr Top Microbiol Immunol 374:53-80.
- Kim JH, O'Brien KM, Sharma R, Boshoff HI, Rehren G, Chakraborty S, Wallach JB, Monteleone M,
   Wilson DJ, Aldrich CC, Barry CE, 3rd, Rhee KY, Ehrt S, Schnappinger D. 2013. A genetic strategy to
   identify targets for the development of drugs that prevent bacterial persistence. Proc Natl Acad
   Sci U S A 110:19095-100.
- 73. Deb C, Lee CM, Dubey VS, Daniel J, Abomoelak B, Sirakova TD, Pawar S, Rogers L, Kolattukudy
   PE. 2009. A novel *in vitro* multiple-stress dormancy model for *Mycobacterium tuberculosis* generates a lipid-loaded, drug-tolerant, dormant pathogen. PLoS One 4:e6077.
- 74. Martini MC, Zhou Y, Sun H, Shell SS. 2019. Defining the transcriptional and post-transcriptional landscapes of *Mycobacterium smegmatis* in aerobic growth and hypoxia. Frontiers in Microbiology 10:591.
- Fan H, Conn AB, Williams PB, Diggs S, Hahm J, Gamper HB, Jr., Hou YM, O'Leary SE, Wang Y, Blaha GM. 2017. Transcription-translation coupling: direct interactions of RNA polymerase with ribosomes and ribosomal subunits. Nucleic Acids Res 45:11043-11055.
- Zhang Y, Mooney RA, Grass JA, Sivaramakrishnan P, Herman C, Landick R, Wang JD. 2014. DksA
   guards elongating RNA polymerase against ribosome-stalling-induced arrest. Mol Cell 53:766-78.
- 629 77. Miller OL, Jr., Hamkalo BA, Thomas CA, Jr. 1970. Visualization of bacterial genes in action. 630 Science 169:392-5.
- 78. Burmann BM, Schweimer K, Luo X, Wahl MC, Stitt BL, Gottesman ME, Rosch P. 2010. A
   NusE:NusG complex links transcription and translation. Science 328:501-4.
- 633 79. Proshkin S, Rahmouni AR, Mironov A, Nudler E. 2010. Cooperation between translating ribosomes and RNA polymerase in transcription elongation. Science 328:504-8.

Tedin K, Bremer H. 1992. Toxic effects of high levels of ppGpp in Escherichia coli are relieved by 635 80. 636 rpoB mutations. J Biol Chem 267:2337-44. 637 Krasny L, Gourse RL. 2004. An alternative strategy for bacterial ribosome synthesis: Bacillus 81. 638 subtilis rRNA transcription regulation. EMBO J 23:4473-83. Stallings CL, Stephanou NC, Chu L, Hochschild A, Nickels BE, Glickman MS. 2009. CarD is an 639 82. 640 essential regulator of rRNA transcription required for Mycobacterium tuberculosis persistence. 641 Cell 138:146-59. 642 83. Esquerre T, Moisan A, Chiapello H, Arike L, Vilu R, Gaspin C, Cocaign-Bousquet M, Girbal L. 2015. Genome-wide investigation of mRNA lifetime determinants in Escherichia coli cells cultured at 643 different growth rates. BMC Genomics 16:275. 644 645 84. Farrow MF, Rubin EJ. 2008. Function of a mycobacterial major facilitator superfamily pump 646 requires a membrane-associated lipoprotein. J Bacteriol 190:1783-91. Snapper SB, Melton RE, Mustafa S, Kieser T, Jacobs WR, Jr. 1990. Isolation and characterization 647 85. 648 of efficient plasmid transformation mutants of Mycobacterium smegmatis. Mol Microbiol 649 4:1911-9. 650 651 652 653 654 655 656

#### FIGURE LEGENDS

Figure 1

658

659

660

661

662

663

664

665

666

667

668

669

670

671

672

673

674

675

676

677

678

679

680

Transcript half-lives are increased in response to hypoxia and carbon starvation stress. (A) Growth kinetics for *M. smegmatis* under hypoxia using a variation of the Wayne model (55), showing OD stabilization at 18-24 hours. Oxygen depletion was assessed qualitatively by methylene blue discoloration. (B) M. smegmatis was sealed in vials to produce a hypoxic environment, at 18 hours transcription was inhibited with RIF and samples collected thereafter. Transcript half-lives for the indicated genes were measured for M. smegmatis mc<sup>2</sup>155 after blocking transcription with 150 µg·mL<sup>-1</sup> RIF. RNA samples were collected (C) during log phase normoxia, and hypoxia (18 hours after closing the bottles); or (D) during log phase in 7H9 supplemented with ADC, glycerol, and Tween 80 (rich media) or 7H9 with Tyloxapol only (carbon starvation, 24 hours). Degradation rates were compared using linear regression (n=3), and half-lives were determined by the reciprocal of the best-fit slope. Error bars: 95% CI. \*\*\* p < 0.001; \*\*\*\* p < 0.0001. When a slope of zero was included in the 95% CI (indicating no degradation), the upper limit for half-life was unbounded, indicated by a clipped error bar with a double line. (E) RIF blocks overexpression of an ATc-inducible gene (rraA) in hypoxic cultures. 40 h after sealing bottles, cultures were treated with 50 ng·mL<sup>-1</sup> ATc and/or 150 μg·mL<sup>-1</sup> RIF or the drug vehicle (DMSO) for 1 h. Expression levels (qPCR) are displayed relative to no drugs (DMSO) treatment. ATc, RIF and DMSO solutions were degassed prior to addition. Error bars: SD.

# Figure 2

Transcript stabilization in hypoxia and carbon starvation is not dependent on the stringent response. (A) Growth kinetics for M. smegmatis mc<sup>2</sup>155 (WT) and  $\Delta rel$ ,  $\Delta sas2$  strains cultured in 7H9 in flasks sealed at time 0. (B) Transcript half-lives for a set of genes 24 hours after sealing the hypoxia bottles (arrow in A). RNA samples were collected after blocking transcription with 150  $\mu$ g·mL<sup>-1</sup> RIF (degassed). (C) Bacteria were grown to log phase in 7H9 supplemented with ADC, glycerol, and Tween 80, then transferred to 7H9 supplemented with Tyloxapol only at time 0. (D) Transcript stability for a set of genes 22 hours after transfer to carbon starvation media (arrow in C). In A and C, the mean and SD of triplicate cultures is shown. In B and D, half-lives were compared using linear regression analysis (n=3). Error bars: 95% CI. \*\*\*\* p<0.0001, n.s. p>0.05. In cases where no degradation was observed or when the upper 95% CI limit was unbounded, the bar or upper error bar were clipped, respectively.

Figure 3

Hypoxia-induced mRNA stability is reversible and independent of mRNA abundance. (A) M. smegmatis was sealed in vials for 18 hours to produce a hypoxic environment, then reexposed to oxygen for two minutes before transcription was inhibited RIF (top) or injected with RIF one minute prior to opening the vials and re-exposing to oxygen (bottom). (B) Transcript half-lives for a set of genes are displayed for log phase normoxia cultures, hypoxia (18 h), and re-aeration with RIF added either before or after opening the vials. Half-lives were compared by linear regression analysis (n=3). (C) Expression levels of transcripts in hypoxia (18 h) or 2 min re-aeration relative to the expression levels in log phase normoxia cultures (percentage). Error bars: SD. (D) Expression levels of transcripts in hypoxia (18 h) or log phase normoxia after

being treated with 200 ng·mL<sup>-1</sup> ATc for 1 h or 10 min, respectively, to induce dCas9 overexpression, relative to the expression levels in a H<sub>2</sub>O vehicle treatment (percentage). Error bars: SD. (E) Transcript half-lives for dCas9 and sigA for log phase normoxia and hypoxia (18 h) after induction of dCas9 with ATc or vehicle treatment as shown in D. In B and E, degradation rates were compared using linear regression (n=3), and half-lives were determined by the reciprocal of the best-fit slope. Error bars: 95% CI. \* p<0.05, \*\* p<0.01, \*\*\*\* p<0.0001, n.s. p>0.05. RIF added to hypoxic cultures was degassed prior to addition.

#### Figure 4

mRNA stability is regulated independently of degradation protein levels. (A) Western blotting for FLAG-tagged RNase E, and c-Myc-tagged PNPase or RNA helicase (msmeg\_1930) in *M. smegmatis* in log phase normoxia, hypoxia (18 h), and 2 min re-aeration. Samples were normalized to total protein level, which were similar on a per-OD basis in all conditions. (B) Translation was inhibited in hypoxic cultures by 150  $\mu$ g·mL<sup>-1</sup> CAM 1 min before adding 150  $\mu$ g·mL<sup>-1</sup> RIF. RNA was harvested at time points beginning 2 min after adding CAM. (C) Transcript half-lives for samples from hypoxic cultures with the drug vehicle (ethanol), hypoxic cultures after translation inhibition, and 2 min re-aeration after translation inhibition. Degradation rates were compared using linear regression (n=3), and half-lives were determined by the reciprocal of the best-fit slope. Error bars: 95% CI. n.s., p>0.05, \* p<0.05, \*\*\*\* p<0.001, \*\*\*\*\* p<0.0001. Drugs and drug vehicles added to the hypoxic cultures were degassed prior to addition.

# Figure 5

727

728

729

730

731

732

733

734

735

736

737

738

739

740

741

742

743

mRNA stability is modulated in response to changes in metabolic status. (A) M. smegmatis was cultured in MMA media for 22 hours to OD<sub>600</sub> 0.8 before being treated with 5 µg·mL<sup>-1</sup> BDQ or the vehicle (DMSO) for 30 min. Intracellular ATP was determined using the BacTiter-Glo kit. (B) Growth kinetics for M. smegmatis from panel A in presence of BDQ. (C) Transcript halflives for a sub-set of transcripts collected during intracellular ATP depletion (30 min with BDQ) or at the basal levels (30 min with DMSO). (D) As in panel A, but for M. smegmatis treated with 500 µg·mL<sup>-1</sup> INH or the vehicle (H<sub>2</sub>O) for 6.5 hours. (E) Growth kinetics for *M. smegmatis* from panel D in presence of INH. (F) Transcript half-lives for a sub-set of transcripts after 6.5 h of INH or vehicle treatment. (G) Growth kinetics for M. smegmatis transitioning into hypoxia, and intracellular ATP levels at different stages. Bottles were sealed at time 0. The dotted line represents the time at which transcript stability analysis were made for the hypoxia (18 h) condition for Figures 1-4. In C and F, half-lives were compared using linear regression analysis (n=3). Error bars: 95% CI. \* p<0.05, \*\* p<0.01, \*\*\* p<0.001, \*\*\*\* p<0.0001. ATP was measured in biological triplicate cultures and is representative of at least two independent experiments.

# 

# **TABLES**

# **TABLE 1**

# 747 Strains used and sources

Strain	Characteristics	Reference or source
mc <sup>2</sup> 155	M. smegmatis, WT	(85)
SS-M_0072	mc <sup>2</sup> 155 derivative transformed with plasmid pSS162, containing an ATc-inducible copy of <i>rraA</i> .	This work
SS-M_0296	mc <sup>2</sup> 155 in which the native copy of RNase E ( <i>rne</i> ) is N-terminally tagged with 6xHis-3xFLAG-TEV-4xGly linker (CACCACCACCACCACCACGATTACAAGGAT CACGATGGCGATTACAAGGATCATGACATC GACTATAAGGACGATGACGATAAGGAGAAC CTGTACTTCCAGGGCGGCGGCGC).	This work
SS-M_0412	SS-M_0296 derivative containing a second copy of PNPase (msmeg_2656) with its predicted native promoter and 5' UTR, and N-terminally tagged with c-Myc-4xGly-linker (GAGCAGAAGCTGATCTCGGAAGAGGACCTC GGCGGCGGCGC) contained on Giles-integrating plasmid pSS282 (Hyg <sup>R</sup> ).	This work
SS-M_0296 derivative containing a second cop RNA helicase (msmeg_1930) with its predicted native promoter and 5' UTR, and C-terminally tagged with 4x Gly linker-c-Myc (GGCGGCGGCGGCGAGCAGAAGCTGATC GA) contained on a Giles-integrating plasmid pSS285 (Hyg <sup>R</sup> ).		This work
$\Delta rel_{ m Msm}$	mc <sup>2</sup> 155 derivative, $\Delta rel \Delta sas 2$	(56)
SS-M_0203	mc <sup>2</sup> 155 derivative transformed with plasmid pJR962, containing an ATc regulated <i>dCas9</i> .	(58)

# **TABLE 2**

# 751 Primers for qPCR

Primer name	Gene	Directionality	Sequence 5' → 3'
SSS903	atpB (msmeg_4942)	Forward	TGTTCGTGTTCGTCTAC
SSS904	<i>atpB</i> (msmeg_4942)	Reverse	CGGCTTGGCGAGTTCTT
SSS909	<i>atpE</i> (msmeg_4941)	Forward	GGGTAACGCGCTGATCTC
SSS910	<i>atpE</i> (msmeg_4941)	Reverse	GAAGGCCAGGTTGATGAAGTA
SSS1241	dCas9	Forward	GACAAGTCGAAGTTCCTGATGTA
SSS1242	dCas9	Reverse	GATCTGCTTGTTCGGGTAGTT
SSS537	<i>esxB</i> (msmeg_0065)	Forward	GGTGAGGACACAGGGAAATAAG
SSS538	<i>esxB</i> (msmeg_0065)	Reverse	CGGAGATGCGCTCGAAAT
SSS856	katG (msmeg_6384)	Forward	GGCCCAATCAGCTCAATCT
SSS857	katG (msmeg_6384)	Reverse	CGGACCGGTAGTCGAAATC
SSS706	<i>rnj</i> (msmeg_2685)	Forward	TCATCCTCTCATCGGGTTTC
SSS707	rnj (msmeg_2685)	Reverse	TTCGCGCTCAACCTTCT
SSS697	rraA (msmeg_6439)	Forward	AACTACGGCGGCAAGAT
SSS698	rraA (msmeg_6439)	Reverse	GTCGAGAGGATCGACTTCAG
JR273 (58)	sigA (msmeg_2758)	Forward	GACTACACCAAGGGCTACAAG
JR274 (58)	sigA (msmeg_2758)	Reverse	TTGATCACCTCGACCATGTG

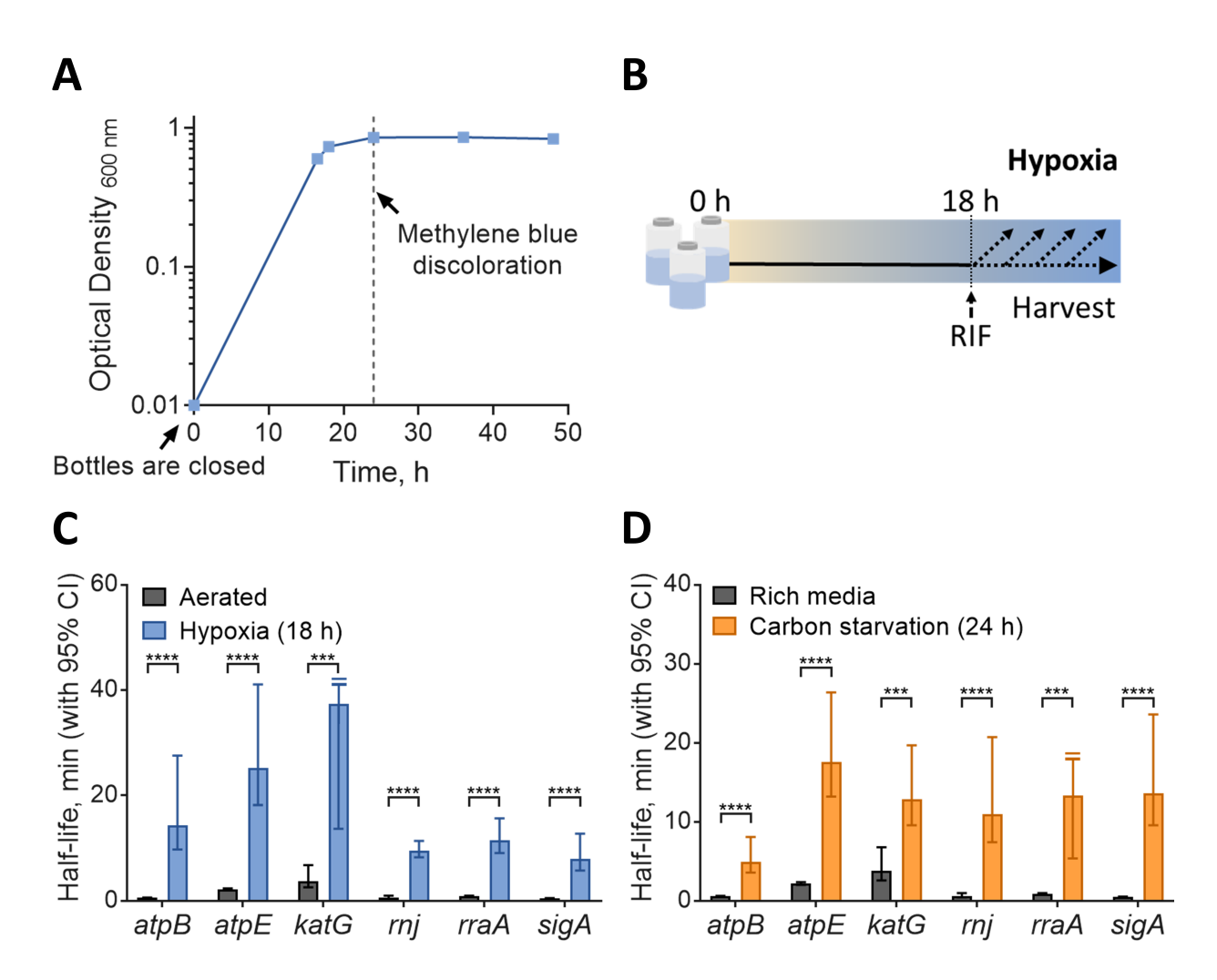
# SUPPLEMENTAL METHODS

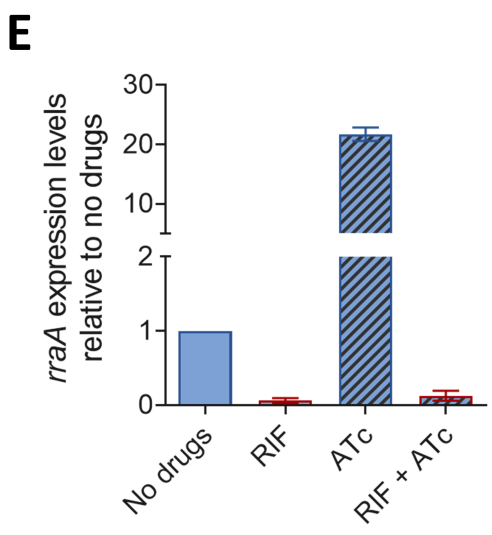
The supplemental methods (Text S1) provide additional detail about the methodology used to measure mRNA half-lives.

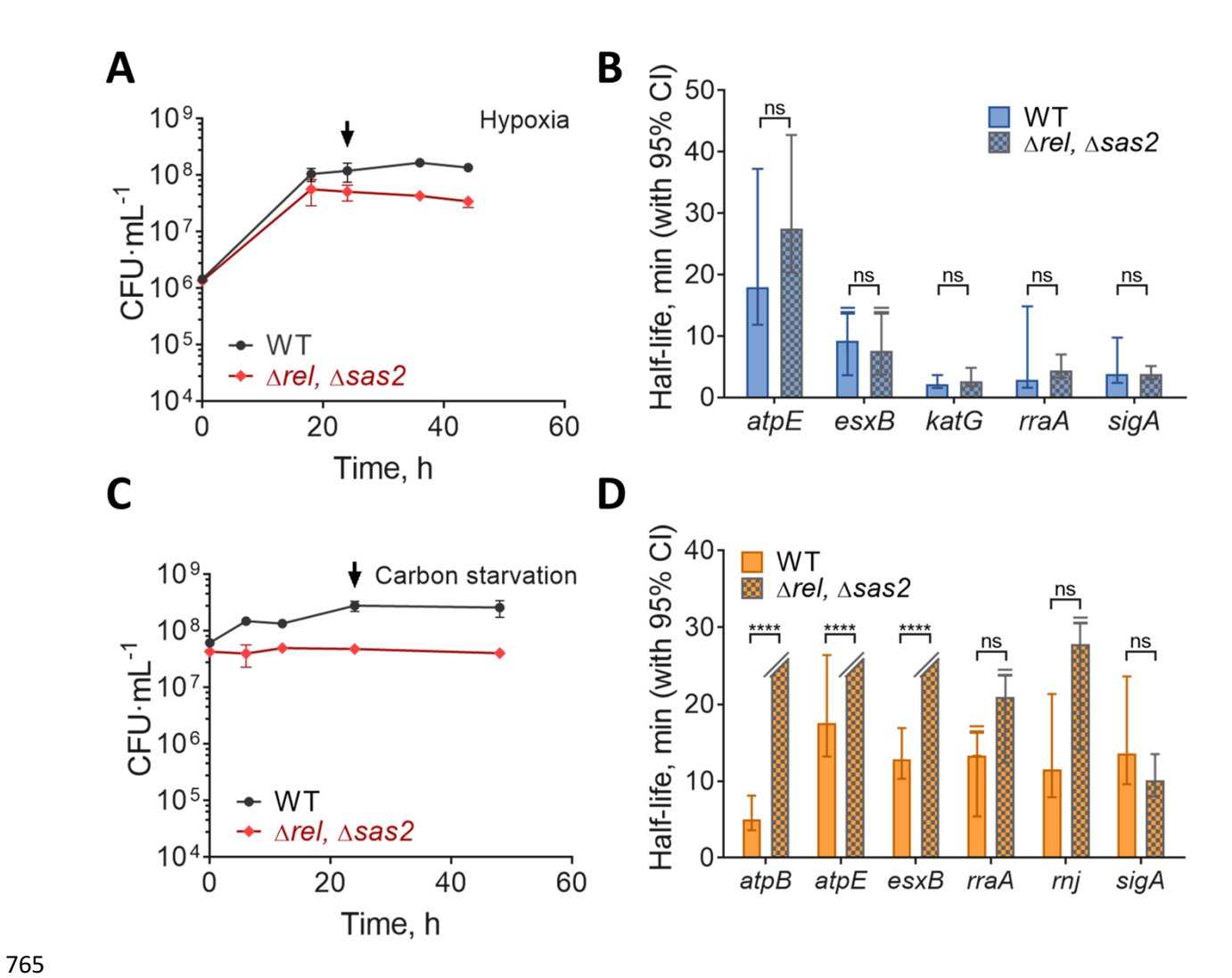
# SUPPLEMENTAL FIGURE LEGENDS

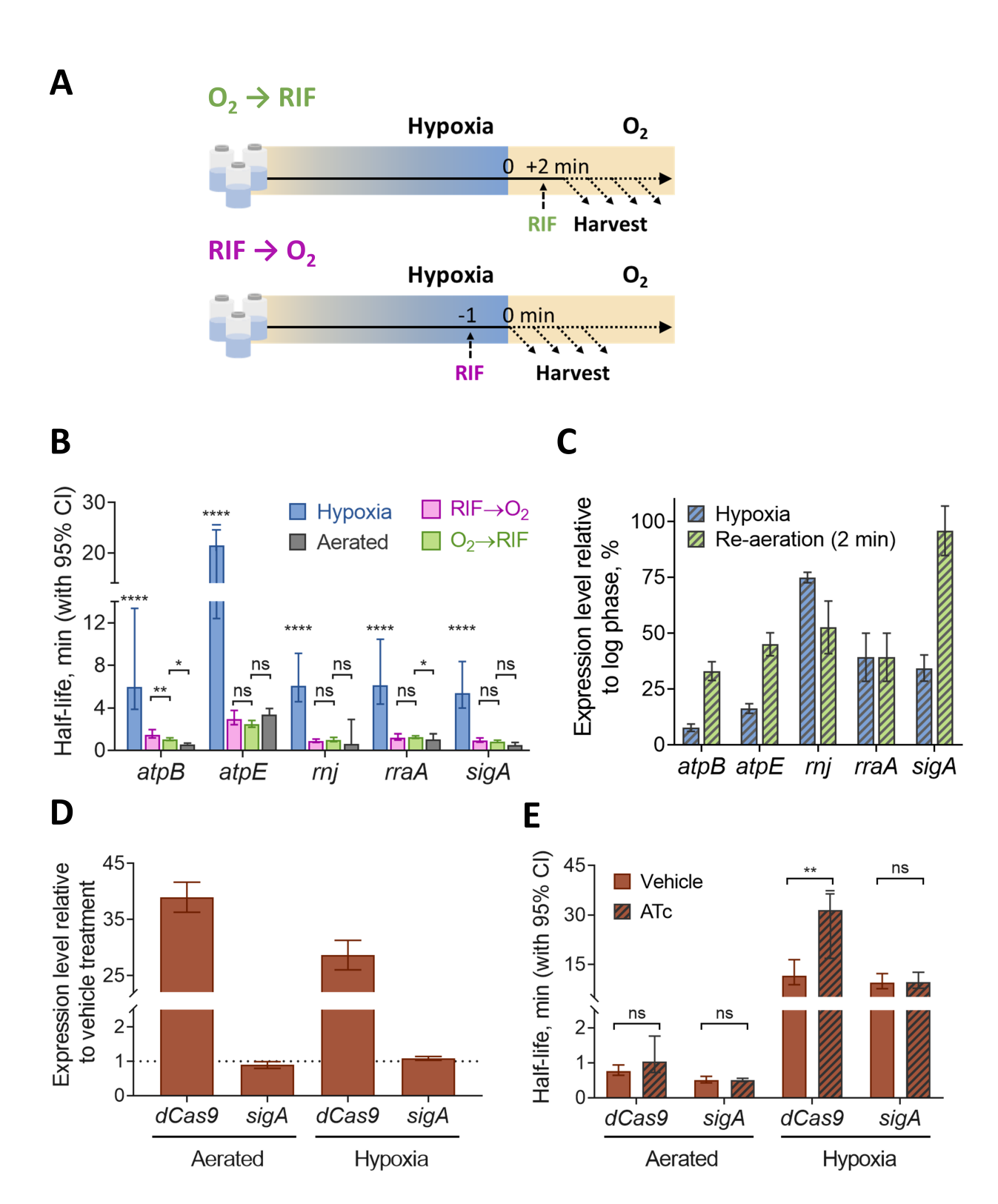
# Supplemental Figure 1

**mRNA** decay curves for an example gene, *rraA*. x axis denotes time after transcription was blocked by addition of RIF. (A) –C<sub>T</sub> versus time data for *rraA* giving a half-life estimate of 0.935 minutes. (B) Estimated mRNA abundance for *rraA* relative to the time of RIF addition, giving a half-life estimate of 0.935 minutes.









# Α

